SINUOUS RILLE SOURCE DEPRESSION MORPHOLOGY AS AN INDICATOR OF LUNAR VOLCANIC ERUPTION CONDITIONS.

Lionel Wilson[1,2] and James W. Head[2] (abstract #1390)
[1]Lancaster Environment Centre, Lancaster University, Lancaster LA1 4YQ, U.K. (l.wilson@lancaster.ac.uk),
[2]Department of Earth, Environmental & Planetary Sciences, Brown University, Providence, RI 02912, U.S.A. (James_Head@brown.edu)

Introduction: We analyze six continuously unroofed sinuous rille channels connected to distinctive source depressions (Table 1; Fig. 1). We previously showed [1-4] how the source depression, like the channel, is caused by erosion of the pre-existing surface by the turbulent flow of hot, low-viscosity lava [5-9]. Here we show that the radius of the source depression is an index of the released volatile content of the erupting magma and that the plan-view shape of the source depression and the presence or absence of positive topography at its outer edge are an index of the mass flux of magma from the vent. Combining magma volatile content with magma eruption rate places rille-forming eruptions within the spectrum of theoretically predicted lunar eruption scenarios [10].

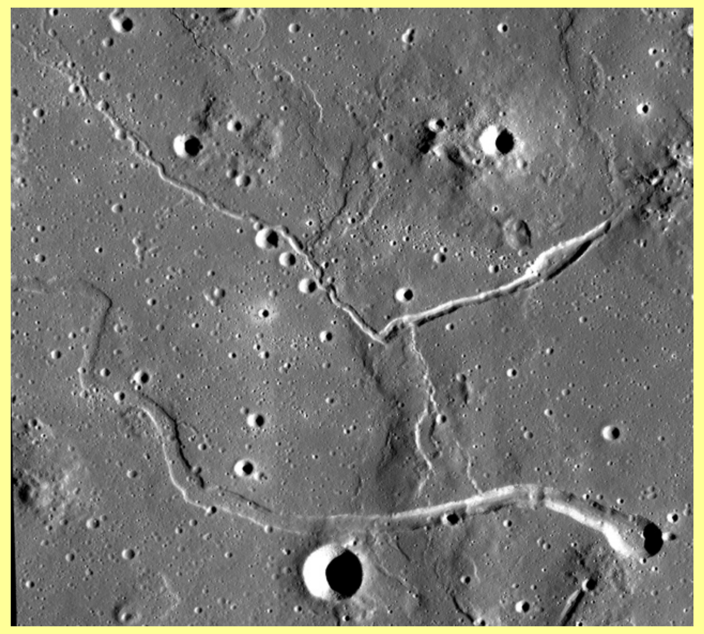

Fig. 1. Examples of the sinuous rilles analyzed, nos. 3 and 4 in Table 1.

Table 1. Locations of the rilles studied. Rille numbers from NASA TM X-62,088.

lat.	lon.	rille no.
13.7	-55.9	3
14.2	-56.0	4
26.3	-43.7	5 (inner)
26.3	-43.7	5 (outer)
26.7	-42.9	6
26.7	-43.2	7

Theory (1): Explosive volcanic eruptions in the lunar vacuum produce umbrella-shaped fire fountains [11]. An optically dense core grades into a transparent outer shell of radial extent X (see Fig. 2a). For a point-source vent forming a circularly-symmetric fountain,

$$X = (6.17\, d\, g^{1/2}\, R^{5/2}) / F \qquad (1)$$

where d is the mean pyroclast diameter, ~300 μm [12], F is the total erupted dense rock equivalent volume flux, R is the maximum range reached by the pyroclasts at the outer edge of the fountain and g is the acceleration due to gravity. For a fissure vent erupting actively for a distance L along strike (Fig. 2b)

$$X = (0.52\, d\, g^{1/2}\, R^{3/2}\, L) / F \qquad (2)$$

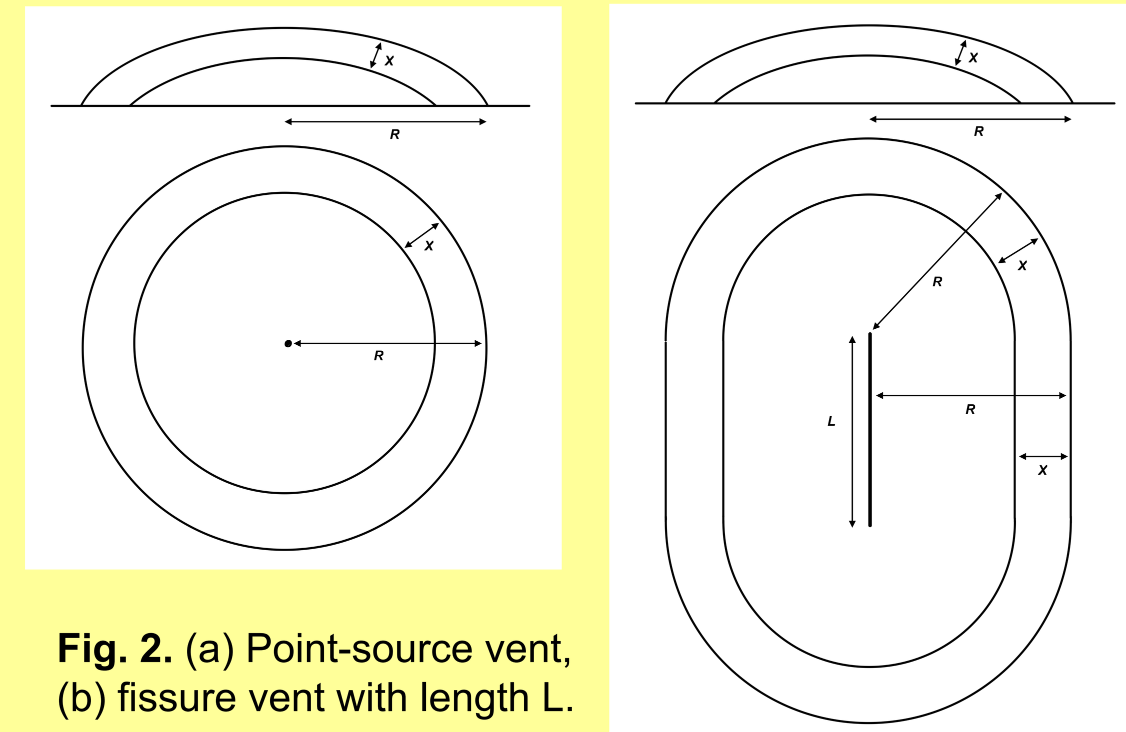

Fig. 2. (a) Point-source vent, (b) fissure vent with length L.

Theory (2): The maximum ballistic pyroclast range R is proportional to the square of the eruption speed, in turn proportional to the released volatile content n of the erupting magma. For volatiles dominated by similar amounts of CO and H_2O [13], the relationship [11] is

$$R = K\, n \qquad (3)$$

where n is the mass fraction of the eruption products that consists of the released gases and $K = 3.98 \times 10^6$ meters (so 1000 ppm, equal to a mass fraction of 10^{-3}, corresponds to R = 3.98 km).

Analysis (1): Values of R and L were compiled for the source depressions of the rilles listed in Table 1 and equation (3) was used to estimate volatile contents, n, for the magmas involved: Table 2. We find n lies in the range 140-513 ppm, placing these eruptions in the lower part of the range of likely lunar volatile contents [13].

Table 2. Maximum pyroclast range, R, fissure length, L, and magma volatile content, n, for rilles studied.

rille no.	R/m	L/m	n/ppm
3	905	740	226
4	560	2940	140
5 (inner)	900	n/a	225
5 (outer)	2050	1020	513
6	1300	n/a	325
7	990	1830	248

Analysis (2): We extend the sinuous rille formation models of [5-9] to include the evolving rheology of the lava eroding the rille channel. Magma erupted at a temperature close to its liquidus is Newtonian and flows in a turbulent manner as it leaves the lava pond around the vent. The lava surface cools by radiation, but efficient mixing of cooled lava with the flow interior means makes the flow near-isothermal. Bulk cooling causes crystal formation which induces non-Newtonian behavior. The viscosity and the yield strength of the lava increase with time and distance from the vent.

We compute the Reynolds and Hedström numbers of the lava as they change along the flow. As the Hedström number increases, the critical Reynolds number to allow turbulence increases, while the actual Reynolds number, initially very large, decreases. When the two become equal, turbulence and thermal erosion stop. We fit the computed variation of rille depth with distance from the vent to the measured depth variation to obtain the magma volume flux, F, the volume of lava erupted, V, and the eruption duration, T, shown in Table 1. The resulting values of X implied by equation (1) and (2), together with the values of F, V and T, are given in Table 3. The entries for rilles 5 (outer) and 7 are shown in italics, as these are the least reliable: rille 5 (outer) is the outer Prinz rille, whose channel floor has been modified by the later 5 (inner) rille [9], and rille 7 has a poorly-defined source depression with an irregular shape (see Fig. 1.).

Table 3. Transparent outer shell of fire fountain thickness, X, lava volume eruption rate, F, lava volume erupted, V, and eruption duration, T, for rilles studied.

rille no.	X/m	F/(m^3 s^{-1})	V/km^3	T/days
3	0.13	29900	101	39
4	0.55	14000	21	17
5 (inner)	*2.54*	*22500*	*67*	*34*
5 (outer)	0.11	169000	537	37
6	5.59	25700	81	37
7	*0.19*	*60700*	*347*	*66*

Results:

(a) Discarding the least reliable results, magma volume eruption rates for rille-forming eruptions average ~2×10^4 m^3 s^{-1}.

(b) Eruption durations lie between 17 and 39 days.

(c) Erupted dense rock equivalent magma volumes range from ~20 to ~100 km^3.

(d) The thicknesses of the cool outer shells of the fire fountains are extremely small, ~0.1 to 5 meters at the edges of fountains with radii of 500 to 1000 m.

Discussion: Fire fountain eruptions on Earth commonly produce a lava pond enclosed by a cinder- or spatter-cone formed from the coolest clasts at the outer edge of the fountain. This analysis predicts that, in the case of lunar rille-forming explosive eruptions, where a lava pond feeds the flow eroding the channel, the very small sizes of lunar pyroclasts cause almost all of the fire fountain to be optically opaque, preventing radiative heat loss. The amount of pyroclastic material at the outer edge of the fountain accumulating cold enough to form an edifice enclosing the lava pond is entirely negligible. This is consistent with the lack of positive topography surrounding the source depressions of sinuous rilles, as seen, for example, in Fig. 2

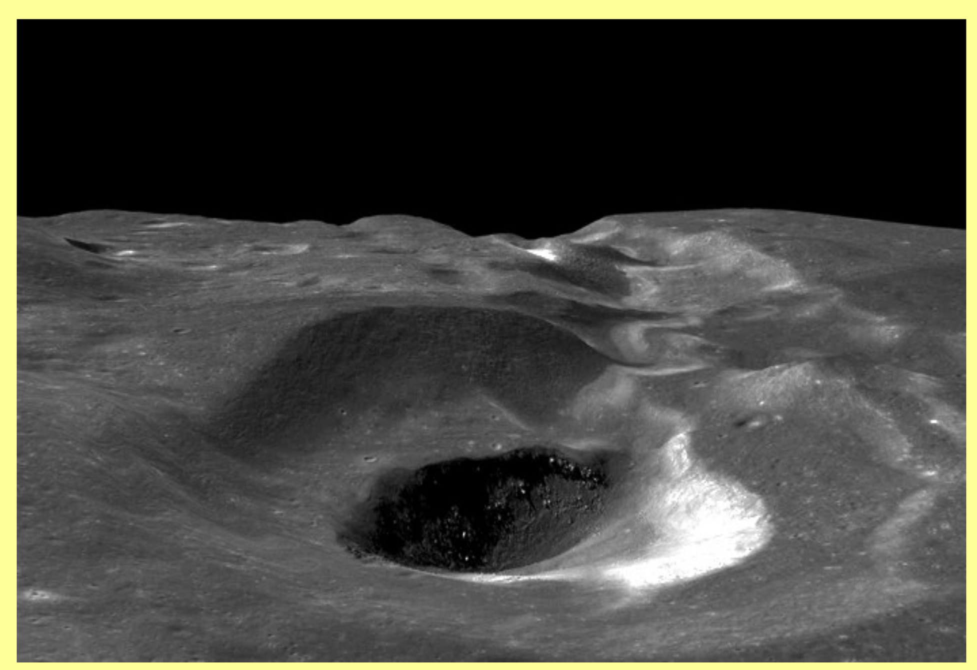

Fig. 3. The source depressions of the inner and outer Prinz rilles, catalog no. 3 in Tables 1-3.

Conclusions: (a) Sinuous rille-forming eruptions involve volumes of low volatile-content basaltic magma that are at the lower end of the volume range needed to ensure complete penetration of a dike through the low-density lunar crust allowing the eruption of a significant volume of magma [11].

(b) Erupted volume fluxes between 10^4 and 10^5 m^3 s^{-1} and eruption durations of a few weeks lie in the range that would be classed as Phase 3 of an eruption forming a long mare lava flow in the eruption evolution scheme of [10].

(c) The reason that an eroded channel, rather than a long positive-topography lava flow, is formed in these eruptions appears to lie in a combination of factors: the magma erupted has an unusually high temperature and therefore a low initial yield strength. Also sinuous rilles tend to form on relatively steep topography, as noted by [14].

(d) These factors together allow turbulence to persist for many tens of kilometers before cooling drives an increasing crystal content high enough to produce a yield strength large enough to force a transition to laminar flow, at which point erosion of the substrate becomes negligible.

References: [1] Head J.W. & Wilson L. (1980) *LPS XI*, 426-428. [2] Wilson L. & Head J.W. (1980) *LPS XI*, 1260-1262. [3] Head J.W. & Wilson L. (1981) *LPS XII*, 427-429. [4] Wilson L. & Head J.W. (2010) *LPS XLI*, #1101. [5] Hulme G. (1973) *Mod. Geol.*, *4*, 107-117. [6] Hulme G. (1982) *Geophys. Surv.*, *5*, 245-279. [7] Williams D.A. et al. (1998) *JGR*, *103*, p. 27,533. [8] Williams D.A. et al. (2000) *JGR*, *105*, p. 20,189. [9] Hurwitz D.M. et al. (2012) *JGR - Planets, 117*, E00H14. [10] Wilson L. & Head J.W. (2018) *GRL, 45*, 5852-5859. [11] Wilson L. & Head J.W. (2017) *Icarus, 283*, 146-175. [12] Morgan C.R., Wilson L. & Head J.W. (2019) *LPS L*, #1341. [13] Rutherford M.J. et al. (2017) *Amer. Mineral., 102*, 2045-2053. [14] Hulme G. & Fielder G. (1977) *Phil. Trans. Roy. Soc. A 285*, 227-234.